

Editorial Manager(tm) for Journal of Zhejiang University-SCIENCE A
Manuscript Draft

Manuscript Number:

Title: Hydromagnetic mixed convection stagnation point flow with radiative heat and mass transfer past a vertical plate embedded in a porous medium

Article Type: Article

Corresponding Author: Oluwole Daniel Makinde, PhD

Corresponding Author's Institution: Cape Peninsula University of Technology

First Author: Oluwole Daniel Makinde, PhD

Order of Authors: Oluwole Daniel Makinde, PhD; Philip Olanrewaju, PhD

Abstract: A study has been carried out to obtain the solutions for hydromagnetic mixed convection stagnation point flow with radiative heat and mass transfer past a vertical plate embedded in a porous medium. The governing two dimensional equations are transformed using a similarity transformation and then solved numerically by shooting method coupled with Runge-Kutta iteration technique. Comparison with previously published work is performed and full agreement is obtained. A parametric study illustrating the influence of the magnetic field parameter, thermal radiation parameter, thermal Grashof number, Grashof numbers, Prandtl number, Schmidt number, on the velocity, temperature, and concentration field as well as the local friction coefficient, the local Nusselt number and the Sherwood number is carried out. The results are illustrated graphically and in tabular form to depict special features of the solutions.

1
2
3
4 **Hydromagnetic mixed convection stagnation point flow with radiative heat and mass**
5 **transfer past a vertical plate embedded in a porous medium**
6
7
8
9

10 **O. D. Makinde¹ and P. O. Olanrewaju²**

11 ¹Institute for Advance Research in Mathematical Modelling and Computations, Cape peninsula University of
12 Technology, P. O. Box 1906, Bellville 7535, South Africa. (E-mail: makinded@cput.ac.za)

13 ²Department of Mathematics, Covenant University, Ota, Ogun State, Nigeria. (E-mail: oladapo_anu@yahoo.ie)
14

15
16
17
18 **Abstract**

19 A study has been carried out to obtain the solutions for hydromagnetic mixed convection stagnation point
20 flow with radiative heat and mass transfer past a vertical plate embedded in a porous medium. The
21 governing two dimensional equations are transformed using a similarity transformation and then solved
22 numerically by shooting method coupled with Runge-Kutta iteration technique. Comparison with
23 previously published work is performed and full agreement is obtained. A parametric study illustrating
24 the influence of the magnetic field parameter, thermal radiation parameter, thermal Grashof number,
25 Grashof numbers, Prandtl number, Schmidt number, on the velocity, temperature, and concentration field
26 as well as the local friction coefficient, the local Nusselt number and the Sherwood number is carried out.
27 The results are illustrated graphically and in tabular form to depict special features of the solutions.
28
29
30
31
32
33
34
35

36 **Keywords:** Volumetric heat generation/absorption; Porous media; Heat and mass transfer; thermal
37 radiation; Stagnation point flow; Mixed convection.
38
39

40 **Nomenclature**

41 g	gravitational acceleration	42 G_T	thermal Grashof number
43 (x, y)	Cartesian coordinates	43 C_w	plate surface concentration
44 C_∞	free stream concentration	44 C	fluid chemical species concentration
45 D	diffusion coefficient	45 f	dimensionless stream function
46 Nu	Nusselt number	46 T_∞	free stream temperature
47 \tilde{K}	porous media permeability	47 G_c	solutal Grashof number
48 Sh	Sherwood number	48 K	permeability parameter
49 T	fluid temperature	49 Pr	Prandtl number
50 T_w	plate surface temperature	50 S	heat generation/absorption parameter
51 k	thermal conductivity coefficient	51 Sc	Schmidt number
52 (u, v)	velocity components	52 Q	volumetric heat generation/absorption rate
53 K'	mean absorption coefficient	53 Ra	thermal radiation parameter
54 B_0	magnetic field of constant strength		

Greek Letters

β^*	coefficient of expansion with concentration
β	coefficient of thermal expansion
μ	coefficient of viscosity
ρ	density of fluid
ϕ	dimensionless concentration
θ	dimensionless temperature
η	dimensionless variable
ν	kinematic viscosity
Ψ	stream function
σ^*	Stefan-Boltzmann constant
σ_e	fluid electrical conductivity

1. Introduction

Hydromagnetic mixed convection flows past a surface embedded in a saturated porous medium have received considerable attention because of numerous applications in engineering and geophysics [1]. Moreover, mixed convection flow of an electrically conducting fluid over a flat surface in the presence of a magnetic field is also of special technical significance because of its frequent occurrence in many industrial applications such as cooling of nuclear reactors, MHD marine propulsion, electronic packages, micro electronic devices etc. Some other quite promising applications are in the field of metallurgy such as MHD stirring of molten metal and magnetic-levitation casting. The analysis of hydromagnetic flows in porous media has been the subject of several recent papers [2-4]. Most of the published papers on convection in porous media under the action of a magnetic field deal with external flows, however, stagnation points do exist at the surface of objects in the flow field, where the fluid is brought to rest by the object. Considerable attention has been given to the study of 2-D stagnation point flow [5, 6]. Hiemenz [7] derived an exact solution of the steady flow of a Newtonian fluid impinging orthogonally on an infinite plane. Ishak et al. [8] investigated mixed convection boundary layers in the stagnation-point flow toward a stretching vertical sheet. Singh et al. [9] studied the effect of volumetric heat generation/absorption on mixed convection stagnation point flow on an iso-thermal vertical plate in porous media.

Meanwhile, thermal radiation is a characteristic of any flow system at temperatures above the absolute zero and can strongly interact with convection in many situations of engineering interest. The influence of radiation on mixed convection is generally stronger than that on forced convection because of the inherent coupling between the temperature and flow fields [10]. Chamkha et al. [11] analyzed the effect of

1
2
3
4 radiation heat transfer on flow and thermal field in the presence of magnetic field for horizontal and
5 inclined plates. The effect of thermal radiation on the heat and mass transfer flow of a variable viscosity
6 fluid past a vertical porous plate permeated by a transverse magnetic field was reported by Makinde and
7 Ogulu [12]. The hydromagnetic flow in the presence of radiation has been investigated by Bestman and
8 Adiepong [13], Naroua et al. [14] and Ouaf [15] when the induced magnetic field is negligible. Raptis et
9 al. [16] investigated the effects of radiation in an optically thin gray gas past a vertical infinite plate in the
10 presence of a magnetic field, when the magnetic Reynolds number is not negligible and the flow is
11 steady.

12
13
14
15
16
17 Our objective in this present study is to extend the recent work of Singh et al. [9] to include
18 hydromagnetic mixed convection stagnation point flow with thermal radiation past a vertical plate
19 embedded in a porous media. The governing boundary-layer equations have been transformed to a two-
20 point boundary value problem in similarity variables, and these have been solved numerically. The effects
21 of various embedded parameters on fluid velocity, temperature and concentration have been shown
22 graphically. It is hoped that the results obtained will not only provide useful information for applications,
23 but also serve as a complement to the previous studies.

2. Mathematical Model

24
25
26
27
28
29
30
31
32
33 Consider steady laminar stagnation point flow of a viscous incompressible electrically conducting fluid
34 through a porous medium along a vertical isothermal plate in the presence of volumetric rate of heat
35 generation and magnetic field. It is assumed that the fluid property variations due to temperature and
36 chemical species concentration are limited to fluid density. In addition, there is no applied electric field
37 and all of the Hall effects and Joule heating are neglected. Since the magnetic Reynolds number is very
38 small for most fluid used in industrial applications, we assume that the induced magnetic field is
39 negligible. The x -axis is taken along the plate and y -axis is normal to the plate and the flow is confined in
40 half plane $y > 0$ as shown in Fig. 1. The potential flow arrives from the y -axis and impinges on plate,
41 which divides at stagnation point into two streams and the viscous flow adheres to the plate. The velocity
42 distribution in the potential flow is given by $U_{\infty} = cx$, where c is a positive constant.

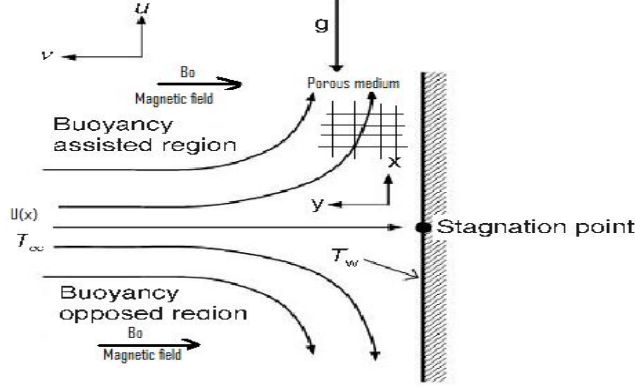


Figure 1. Schematic diagram of the problem

Following [5-9] the linear Darcy term representing distributed body force due to porous media is retained while the non-linear Forchheimer term is neglected, thus the governing equations of continuity, momentum, energy and species concentration are given by

$$\frac{\partial u}{\partial x} + \frac{\partial v}{\partial y} = 0, \quad (1)$$

$$u \frac{\partial u}{\partial x} + v \frac{\partial u}{\partial y} = \nu \frac{\partial^2 u}{\partial y^2} + g\beta(T - T_\infty) + g\beta^*(C - C_\infty) - \frac{\sigma_e B_0^2}{\rho}(u - U_\infty) - \frac{\nu}{\tilde{K}}(u - U_\infty) + U_\infty \frac{dU_\infty}{dx}, \quad (2)$$

$$u \frac{\partial T}{\partial x} + v \frac{\partial T}{\partial y} = \alpha \frac{\partial^2 T}{\partial y^2} - \frac{\alpha}{k} \frac{\partial q_r}{\partial y} + Q(C - C_\infty), \quad (3)$$

$$u \frac{\partial C}{\partial x} + v \frac{\partial C}{\partial y} = D \frac{\partial^2 C}{\partial y^2}. \quad (4)$$

The boundary conditions are

$$\begin{aligned} u=0, v=0, T=T_w, C=C_w \text{ at } y=0, \\ u \rightarrow U_\infty = cx, T \rightarrow T_\infty, C \rightarrow C_\infty \text{ as } y \rightarrow \infty, \end{aligned} \quad (5)$$

where u and v are the velocity components in the x - and y -directions, respectively, ρ is the fluid density, ν is the kinematic viscosity, σ_e is the electrical conductivity of the fluid, \tilde{K} is the permeability of the porous medium, g is the gravitational acceleration, β is the thermal expansion coefficient, β^* is the coefficient of expansion with concentration, T is the temperature, c_p is the specific heat capacity at constant pressure of the fluid, α is the thermal diffusivity of the fluid, k is thermal conductivity, T_w is the temperature of the plate, Q is the volumetric rate heat generation/absorption, B_0 is the magnetic field of constant strength and D is the coefficient of mass diffusivity. Using the Rosseland approximation, the radiative heat flux in the y -direction is given by Sparrow and Cess [10],

$$q_r = -\frac{4\sigma^*}{3K'} \frac{\partial T^4}{\partial y}, \quad (6)$$

where σ^* and K' are the Stefan-Boltzmann constant and the mean absorption coefficient, respectively. As done by Makinde and Ogulu [12], temperature differences within the flow are assumed to be sufficiently small so that T^4 may be expressed as a linear function of temperature T using a truncated Taylor series about the free stream temperature T i.e.

$$T^4 \approx 4T_\infty^3 T - 3T_\infty^4. \quad (7)$$

We introduce the following non-dimensional variables:

$$\begin{aligned} \eta = y\sqrt{\frac{c}{\nu}}, \psi(x, y) = \sqrt{\nu c} x f(\eta), \theta(\eta) = \frac{T - T_\infty}{T_w - T_\infty}, \phi(\eta) = \frac{C - C_\infty}{C_w - C_\infty}, \\ G_T = \frac{g\beta(T_w - T_\infty)x^3}{\nu^2}, G_c = \frac{g\beta(C_w - C_\infty)x^3}{\nu^2}, Ra = \frac{4\sigma^* T_\infty^3}{kK'}, Re = \frac{U_\infty x}{\nu}, \\ K = \frac{\nu}{c\tilde{K}}, Pr = \frac{\nu}{\alpha}, Sc = \frac{\nu}{D}, \nu = \frac{\mu}{\rho}, M = \frac{\sigma_e B_0^2}{c\rho}, S = \frac{Q(C_w - C_\infty)\nu}{c\alpha(T_w - T_\infty)}, \end{aligned} \quad (8)$$

where ψ is the stream function which is defined in the usual form as $u = \partial\psi/\partial x$ and $v = -\partial\psi/\partial y$ so that the continuity equation (1) is automatically satisfied. Substituting the expression in Eq. (7) together with the similarity variables in Eq. (8) into Eqs. (1)-(5), we obtain the following nonlinear ordinary differential equations:

$$f''' + ff'' - f'^2 + G_T\theta + G_c\phi - (K + M)(f' - 1) + 1 = 0, \quad (9)$$

$$\left(1 + \frac{4}{3}Ra\right)\theta'' + Pr f\theta' + S\phi = 0, \quad (10)$$

$$\phi'' + Scf\theta' = 0, \quad (11)$$

where K is the porous medium permeability parameter, Ra is the thermal radiation parameter, G_T is the local thermal Grashof number, G_c is the local solutal Grashof number, Pr is the Prandtl number, Sc is the Schmidt number, M is the magnetic field intensity parameter and S is the rate of heat generation/absorption parameter. The corresponding boundary conditions (5) now becomes

$$\begin{aligned} f = 0, \quad f' = 0, \quad \theta = 1, \quad \phi = 1 \quad \text{at} \quad \eta = 0, \\ f' = 1, \quad \theta = 0, \quad \phi = 0 \quad \text{as} \quad \eta \rightarrow \infty. \end{aligned} \quad (12)$$

The set of equations (9)–(11) under the boundary conditions (12) have been solved numerically by applying the Nachtsheim and Swigert [17] shooting iteration technique together with Runge-Kutta sixth-order integration scheme. From the process of numerical computation, the skin-friction coefficient, the local Nusselt number and the local Sherwood number, which are respectively given by

$$C_f = 2(Re)^{-1/2} f''(0), \quad Nu = -(Re)^{1/2} \theta'(0), \quad Sh = -(Re)^{1/2} \phi'(0), \quad (13)$$

are also worked out and their numerical values are presented in a tabular form for each set of parameters embedded in the system. In order to verify the validity of our numerical method, results of the skin-friction coefficient, the local Nusselt number and the local Sherwood number for the case of the boundary layer stagnation flow in the absence of thermal radiation and magnetic field are compared with those reported by Singh *et al.* [9] as illustrated in the table (1) and the results are found to be in excellence agreement.

Table 1: Computations showing the comparison with Singh *et al.* [9] for different values of S when $G_T=1.0, G_c=0.5, Pr = 1, Sc=0.5, M=0, Ra=K=0$.

S	$f''(0)$ [9]	$-\theta'(0)$ [9]	$-\phi'(0)$ [9]	$f''(0)$ Present	$-\theta'(0)$ Present	$-\phi'(0)$ Present
-1	1.8444	1.3908	0.4631	1.844462	1.390856	0.463174
0	1.9995	0.6392	0.4789	1.999553	0.639244	0.478964
1	2.1342	-0.0730	0.4917	2.134287	-0.073040	0.491749

3. Results and Discussions

Here, we focus on the positive values of the buoyancy parameters i.e. Grashof number $G_T > 0$ (which corresponds to the cooling problem) and solutal Grashof number $G_c > 0$ (which indicates that the chemical species concentration in the free stream region is less than the concentration at the boundary surface). The cooling problem is often encountered in engineering applications. From table (2), it is interesting to note that the local skin friction at the plate surface increases with increasing parameter M, S, G_T, G_c, Ra and K and decreases with increasing values of Prandtl number and Schmidt number. This implies that combined effect of buoyancy forces, magnetic field, thermal radiation, internal heat generation and decreasing porous medium permeability is to increase the local skin friction at the plate surface. Similarly, the local Nusselt number (Nu) coefficient at the plate surface increases with an increase in parameter values of $G_T, G_c, M, K,$ and Pr and decreases with an increase in S and Sc . Moreover, it is noteworthy that local Sherwood number (Sh) at the plate surface increases with a combined increase in the internal heat generated in the flow system ($S > 0$) and magnetic intensity ($M > 0$) and decreases with other parameters.

Table 2: Computations showing $f''(0)$, $-\theta'(0)$, $-\phi'(0)$ for various values of embedded parameters

S	K	Pr	G_T	G_C	Sc	M	Ra	$f''(0)$	$-\theta'(0)$	$-\phi'(0)$
-1	1	0.1	1	0.5	0.5	0.1	0.1	1.699972	2.31922	0.249053
0	1	0.1	1	0.5	0.5	0.1	0.1	2.389898	0.236593	0.502813
0.5	1	0.1	1	0.5	0.5	0.1	0.1	2.477113	-0.20393	0.513073
1	3	0.1	1	0.5	0.5	0.1	0.1	2.878166	-0.64378	0.518639
1	5	0.1	1	0.5	0.5	0.1	0.1	3.184808	-0.65098	0.517897
1	1	1	1	0.5	0.5	0.1	0.1	2.370055	-0.04316	0.494804
1	1	10	1	0.5	0.5	0.1	0.1	2.154799	1.073118	0.474395
1	1	0.1	0.5	0.5	0.5	0.1	0.1	2.220679	-0.68158	0.496618
1	1	0.1	0.7	0.5	0.5	0.1	0.1	2.358558	-0.65897	0.507416
1	1	0.1	0.5	1	0.5	0.1	0.1	2.437256	-0.66294	0.507347
1	1	0.1	0.5	2	0.5	0.1	0.1	2.856783	-0.63004	0.526974
1	1	0.1	0.5	0.5	1	0.1	0.1	2.170082	-0.49096	0.653140
1	1	0.1	0.5	0.5	2	0.1	0.1	2.125898	-0.33929	0.851850
1	1	0.1	0.5	0.5	0.5	1	0.1	2.305895	-0.05390	0.859057
1	1	0.1	0.5	0.5	0.5	3	0.1	2.704379	-0.04824	0.879438
1	1	0.1	0.5	0.5	0.5	0.1	1	2.103755	0.006342	0.848097
1	1	0.1	0.5	0.5	0.5	0.1	3	2.104745	0.049987	0.848680

A.) Effects of parameter variation on velocity profiles

Figs. 2-7 demonstrate the effects of various thermophysical parameters on the velocity profiles. Generally, the fluid velocity increases gradually from the stationary plate surface and within the boundary layer region, then converging to its free stream value far away from the plate satisfying the boundary condition. Fig. 2 depicts the effect of parameter S on the fluid velocity and we observed an increase in the fluid velocity as parameter S increases. This is because an increase in the volumetric rate of generation connotes increase in buoyancy force thereby increasing fluid velocity. Fig. 3 depicts the influence of Prandtl number on the velocity profiles. It is interesting to note that increasing Prandtl number increases the fluid velocity. Similar trend is observed in fig. 4 with an increase in Schmitz number. In fig. 6, we observed a decrease in the velocity boundary thickness with an increase in the intensity of magnetic field. Fig. 7, illustrates the effect of thermal radiation absorption on the velocity profiles. An increase in the parameter value of the thermal radiation parameter leads to a further increase in the fluid velocity within the boundary layer region.

1
2
3
4
5
6
7
8
9
10
11
12
13
14
15
16
17
18
19
20
21
22
23
24
25
26
27
28
29
30
31
32
33
34
35
36
37
38
39
40
41
42
43
44
45
46
47
48
49
50
51
52
53
54
55
56
57
58
59
60
61
62
63
64
65

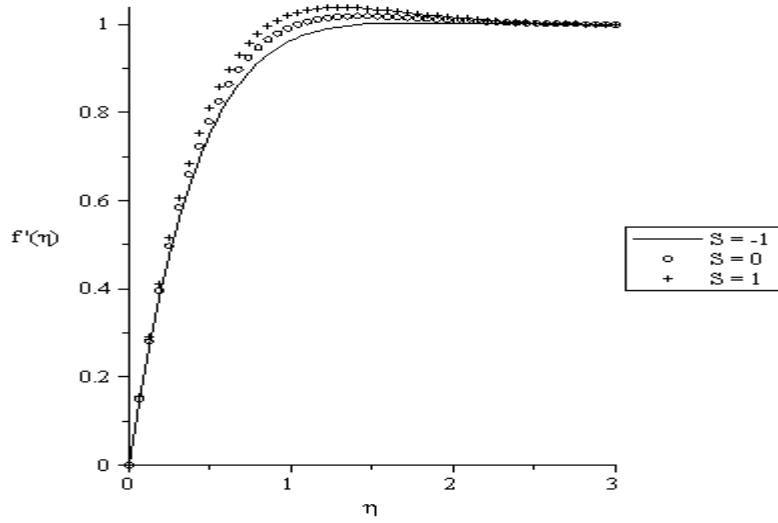


Figure 2: Velocity profiles for $G_T = 1$, $G_c = 0.5$, $K = 0.0$, $Pr = 1$, $Sc = 0.5$, $M = 0.1$, $Ra = 0.1$

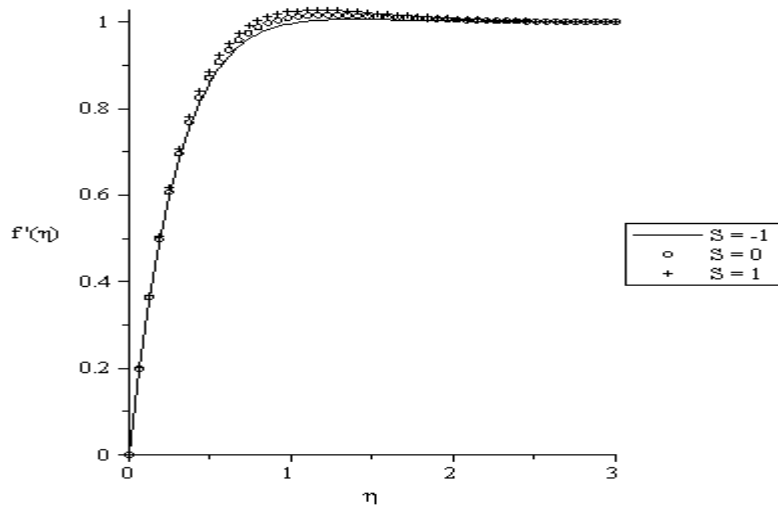


Figure 3: Velocity profiles for $G_T = 1$, $G_c = 0.5$, $K = 5$, $Pr = 1$, $Sc = 0.5$, $M = 0.1$, $Ra = 0.1$

1
2
3
4
5
6
7
8
9
10
11
12
13
14
15
16
17
18
19
20
21
22
23
24
25
26
27
28
29
30
31
32
33
34
35
36
37
38
39
40
41
42
43
44
45
46
47
48
49
50
51
52
53
54
55
56
57
58
59
60
61
62
63
64
65

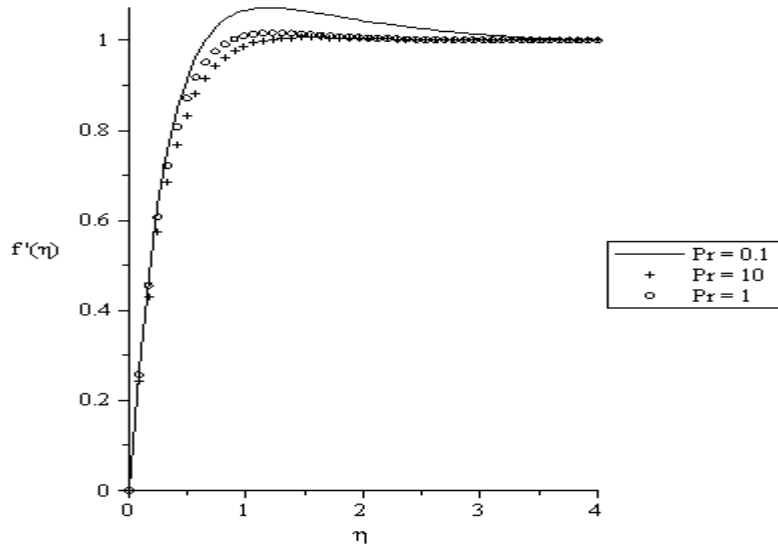


Figure 4: Velocity profiles for $G_T = 1$, $G_c = 0.5$, $K = 5$, $S = 0.0$, $Sc = 0.5$, $M = 0.1$, $Ra = 0.1$

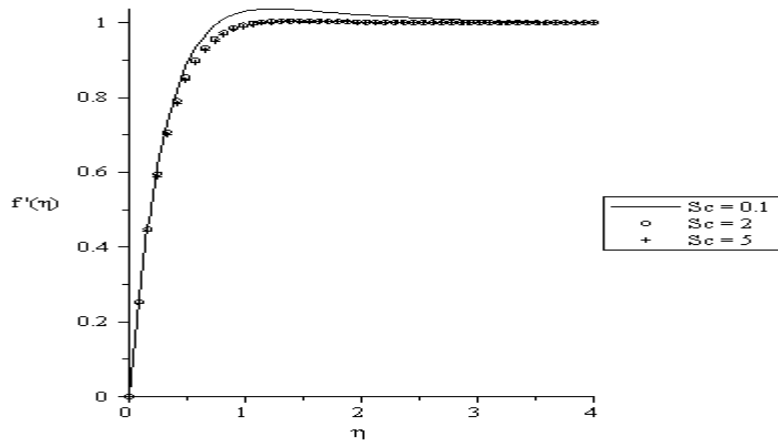


Figure 5: Velocity profiles for $G_T = 1$, $G_c = 0.5$, $K = 5$, $S = 0.0$, $Pr = 1$, $M = 0.1$, $Ra = 0.1$

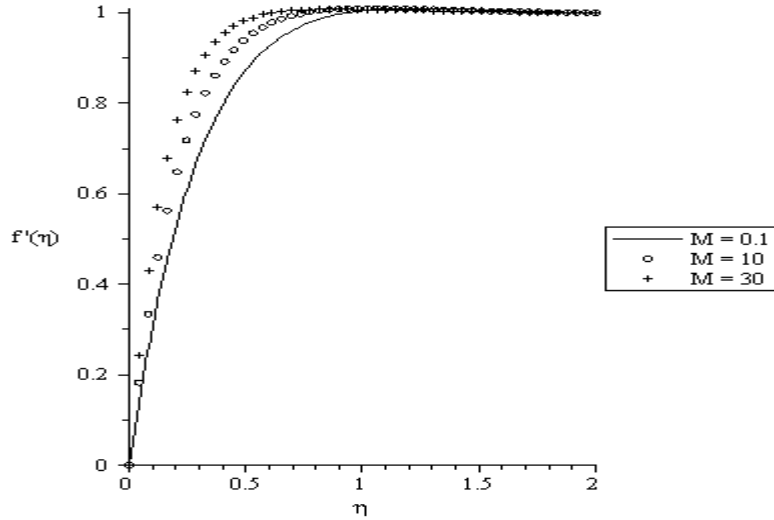


Figure 6: Velocity profiles for $G_T = 1$, $G_c = 0.5$, $K = 5$, $S = 0.0$, $Pr = 1$, $Sc = 0.5$, $Ra = 0.1$

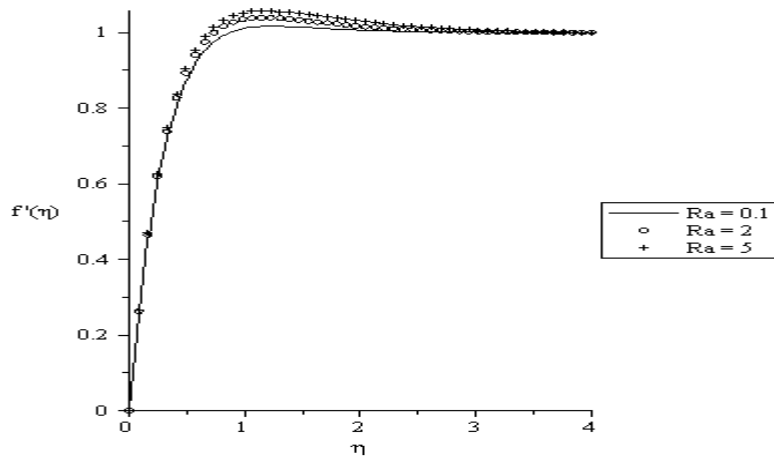


Figure 7: Velocity profiles for $G_T = 1$, $G_c = 0.5$, $K = 5$, $S = 0.0$, $Pr = 1$, $Sc = 0.5$, $M = 0.1$

B. Effects of parameter variation on temperature profiles

Figs. 8 -10 illustrate the temperature field against spanwise coordinate η . The fluid temperature is highest at the plate surface and decreases exponentially to the free stream zero value far away from the plate satisfying the boundary condition. The thermal boundary layer thickness increases with an increase in internal heat generation in the flow field and decreases with heat loss as displayed in Fig. 8. Similar trend is observed in Fig. 9 with an increase in radiative heat generated within the flow field. An increase in the Ra causes an increase in the fluid temperature. In fig. 10, it is seen that increase in Pr brings a decrease in the thermal boundary layer thickness. At high Prandtl number, the fluid has low velocity, which in turn also implies lower thermal diffusivity leading to a decrease in the fluid temperature.

1
2
3
4
5
6
7
8
9
10
11
12
13
14
15
16
17
18
19
20
21
22
23
24
25
26
27
28
29
30
31
32
33
34
35
36
37
38
39
40
41
42
43
44
45
46
47
48
49
50
51
52
53
54
55
56
57
58
59
60
61
62
63
64
65

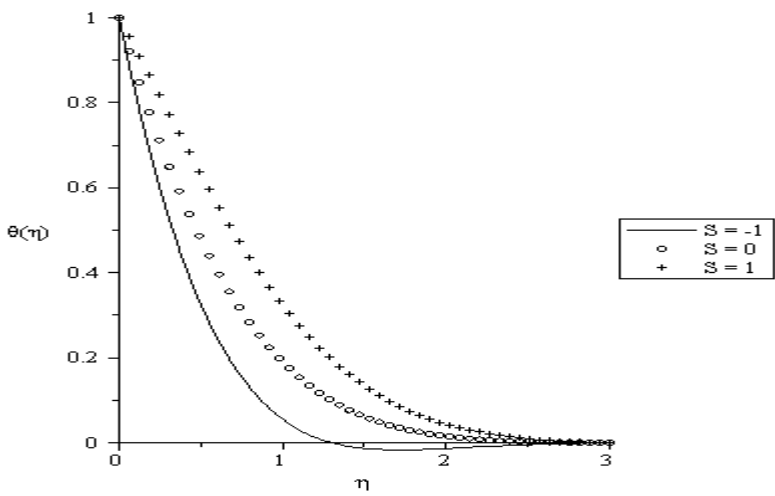


Figure 8: Temperature profiles for $G_T = 1$, $G_c = 0.5$, $K = 5$, $Pr = 1$, $Sc = 0.5$, $M = 0.1$, $Ra = 0.1$

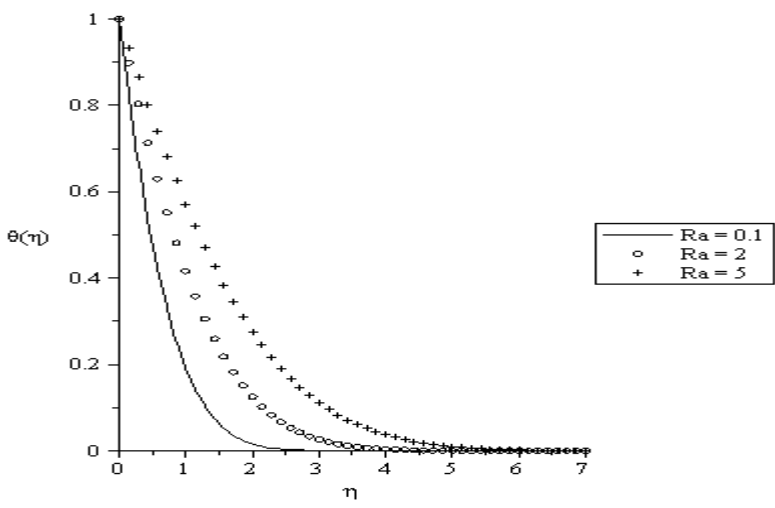


Figure 9: Temperature profiles for $G_T = 1$, $G_c = 0.5$, $K = 5$, $S = 0.0$, $Pr = 1$, $Sc = 0.5$, $M = 0.1$

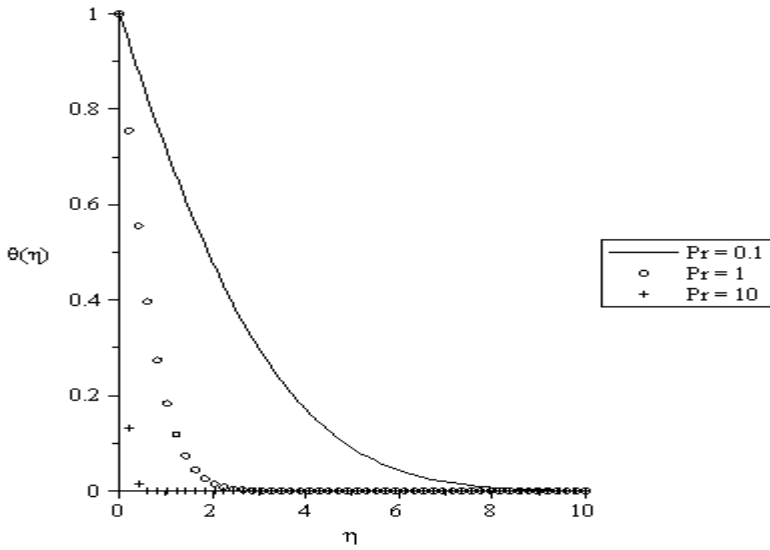


Figure 10: Temperature profiles for $G_T = 1$, $G_C = 0.5$, $K = 5$, $S = 0.0$, $Sc = 0.5$, $M = 0.1$, $Ra = 0.1$

C. Effects of parameter variation on concentration profiles

Figure 12 shows the profiles of the species concentration with the boundary layer. The concentration is highest at the plate surface and decreases exponentially to the free stream zero value far away from the plate. An increase in Schmidt number Sc causes a decrease in the species concentration due to a decrease in the molecular diffusivity of the chemical species at high Schmidt number.

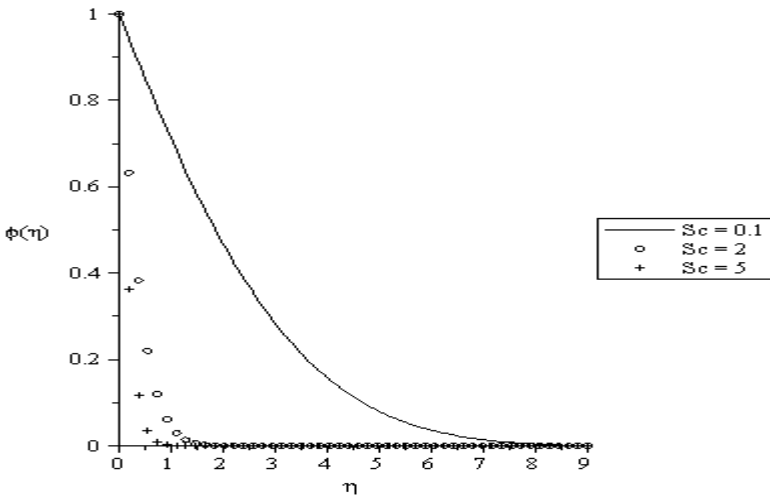


Figure 11: Concentration profiles for $G_T = 1$, $G_C = 0.5$, $K = 5$, $S = 0.0$, $Pr = 1$, $M = 0.1$, $Ra = 0.1$

Conclusions

1
2
3
4 In this paper, the hydromagnetic mixed convection stagnation point flow with thermal radiation over a
5 vertical plate embedded in a porous medium is investigated. The nonlinear boundary layer equations
6 governing the problem are obtained and solved numerically. Pertinent results are displayed graphically
7 and in a tabular form. Our results revealed among many others that:
8
9

- 10 1. The skin-friction, the rate of mass transfer and the rate of heat transfer increases as magnetic field strength
11 M , and radiation parameters Ra increase.
12
- 13 2. The fluid velocity and temperature increases, while the concentration of the species decreases with an
14 increase in the radiation parameter.
15
- 16 3. Increasing the rate of heat generation/absorption parameter S bring an increase in the skin-friction and the
17 rate of mass transfer, while the rate of heat transfer decreases.
18
- 19 4. Fluid velocity and temperature increase while the concentration of the species decreases with the increase
20 in the rate of heat generation/absorption parameter S .
21
22
23
24
25

26 **Acknowledgements**

27 The authors would like to thank Covenant University, Nigeria and National Research Foundation of
28 South Africa for their financial support.
29
30
31
32
33

34 **References**

- 35 [1] D.A. Nield, A. Bejan, Convection in Porous Media, third ed., Springer, New York, 2006.
- 36 [2] M. Kumari, H.S. Takhar, G. Nath, Mixed convection flow over a vertical wedge embedded in a
37 highly porous medium, Heat Mass Transfer 37 (2001) 139–146.
- 38 [3] A.J. Chamkha, M.M.A. Quadri, Heat and mass transfer from a permeable cylinder in a porous
39 medium with magnetic field and heat generation/ absorption effects, Numer. Heat Transfer, Part A 40
40 (2001) 387–401.
- 41 [4] M.A. Seddeek, Effects of magnetic field and variable viscosity on forced non- Darcy flow about a flat
42 plate with variable wall temperature in porous media in the presence of suction and blowing, J. Appl.
43 Mech. Tech. Phys. 43 (2002) 13–17.
- 44 [5] J.T. Stuart, The viscous flow near a stagnation point when the external flow has uniform vorticity,
45 Journal of Aerospace Science and Technology, vol. 26 (1959) 124-125.
- 46 [6] K. Tamada, Two-dimensional stagnation-point flow impinging obliquely on a plane wall, Journal of
47 the Physical Society of Japan, vol. 46 (1979) 310-311.
- 48 [7] K. Hiemenz, Die Grenzschicht in einem in den gleichformigen Flussigkeitsstrom eingetauchten
49 gerade Kreiszyylinder, Dingler Polytechnic Journal, 326 (1911) 321-410.
50
51
52
53
54
55
56
57
58
59
60
61
62
63
64
65

- 1
2
3
4 [8] A. Ishak, R. Nazar, I. Pop, Mixed convection boundary layers in the stagnation-point flow toward a
5 stretching surface, *Meccanica* 41 (2006) 509-518.
6
7 [9] G. Singh, P.R. Sharma, A.J. Chamkha, Effect of volumetric heat generation/absorption on mixed
8 convection stagnation point flow on an Iso-thermal vertical plate in porous media, *Int. J. Industrial*
9 *Mathematics* vol. 2, No. 2 (2010) 59-71.
10
11 [10] E.M. Sparrow, R.D. Cess, *Radiation Heat Transfer*, Augmented edition, Hemisphere Publishing
12 Corp, Washington, DC, 1978.
13
14 [11] A.J. Chamkha, C. Issa, K. Khanfer, Natural convection from an inclined plate embedded in a variable
15 porosity porous medium due to solar radiation, *Internat. J. Therm. Sci.* 41 (2002) 73–81.
16
17 [12] O. D. Makinde, A. Ogulu, The effect of thermal radiation on the heat and mass transfer flow of a
18 variable viscosity fluid past a vertical porous plate permeated by a transverse magnetic field, *Chemical*
19 *Engineering Communications*, 195 (12), (2008) 1575 -1584.
20
21 [13] A.R. Bestman, S.K. Adiepong, Unsteady hydromagnetic free-convection flow with radiative heat
22 transfer in a rotating fluid, *Astrophysics and Space Science* **143**, (1988) pp.73-80.
23
24 [14] H. Naroua, P.C. Ram, A.S. Sambo, H.S. Takhar. Finite-element analysis of natural convection flow
25 in a rotating fluid with radiative heat transfer, *Journal of Magnetohydrodynamics and Plasma Research* 7,
26 (1998) pp.257-274.
27
28 [15] M. E. M. Ouaf, Exact solution of thermal radiation on MHD flow over a stretching porous sheet,
29 *Applied Mathematics and Computation*, 170, 2, (2005) pp. 1117-1125.
30
31 [16]. A. Raptis, C. Perdakis, A. Leontitsis. Effects of radiation in an optically thin gray gas flowing past a
32 vertical infinite plate in the presence of a magnetic field, *Heat and Mass Transfer* **39**, (2003) pp.771-773.
33
34 [17] T.Y. Na, *Computational Methods in Engineering Boundary Value Problems*, Academic Press, New
35 York, 1979.
36
37
38
39
40
41
42
43
44
45
46
47
48
49
50
51
52
53
54
55
56
57
58
59
60
61
62
63
64
65